ChemComm

Ligand Architecture for Triangular Metal Complexes: A High Oxidation State Ni3 Cluster with Proximal Metal Arrangement

Journal:	*ChemComm*
Manuscript ID	CC-COM-05-2020-003816.R1
Article Type:	Communication

COMMUNICATION

Ligand Architecture for Triangular Metal Complexes: A High Oxidation State Ni_3 Cluster with Proximal Metal Arrangement

Manar M. Shoshani and Theodor Agapie*

Received 00th January 20xx,
Accepted 00th January 20xx

DOI: 10.1039/x0xx00000x

A new multidentate tetraanionic ligand platform for supporting trinuclear transition metal clusters has been developed. Two trisphenoxide phosphinimide ligands bind three Ni centers in a triangular arragnement. The phosphinimide donors bridge in μ_3 fashion and the phenoxides complete a pseudo-square planar coordination sphere around each metal center. Electrochemical studies reveal two pseudo-reversible oxidation events at notably low potentials (-0.70 and 0.05 mV). The one electron oxidized species was characterized structurally, and it is assigned as a Ni^{III}-containing cluster.

Multimetallic complexes have been explored for applications including bond formation and cleavage reactions,[1] multi-electron redox processes,[2] and modelling of biological active sites.[3] Elaborate multidentate ligand designs have been employed to rationally control the nuclearity, structure, and properties of metal clusters.[1e, 4] Though there has been significant progress in the synthesis of clusters of predictable structure using multidentate ligand scaffolds, few examples are known pertaining to closely spaced triangular M_3 species.[1e, 4c, d, 5] Trinuclear clusters supported by cyclophane-based motifs perform small molecule activation, including CO_2[6] and N_2[1e] reduction. Trimetallic complexes with an open M_3 face have been shown to facilitate multimetallic redox reactivity.[5c, 7]

In continued efforts to develop synthetic strategies to more highly oxidized metal clusters,[8] we have targeted a multinucleating ligand with high negative charge designed using a phosphinimide motif. Phosphinimide ligands are well established as bridging ligands for multimetallic species and are also known to support high oxidation state metal centers. Recently, phosphinimide ligands have been used to stabilize the +4 oxidation state of a series of lanthanides.[9] Phosphimine and phosphinimide ligands have been employed to stabilize multimetallic species,[1f, 10] taking advantage of the high electron density and donating ability of the nitrogen center.[9b] For examples, phosphinimide ligands bridging in μ_2 fashion have been employed for tetranuclear clusters of Ni and Co that serve as precursors in catalysis.[1f] However, the nuclearity of complexes supported by phosphinimide ligands can vary, including di-, tetra-, and octa-nuclear complexes, while the metal binding mode can be terminal, μ_2 , or μ_3 (Figure 1).[1f, 11] To control the nuclearity resulting from phosphinimide ligands, we sought to form trinuclear clusters using additional donors to enforce metal-binding upon bridging by a phosphinimide (Figure 1b).

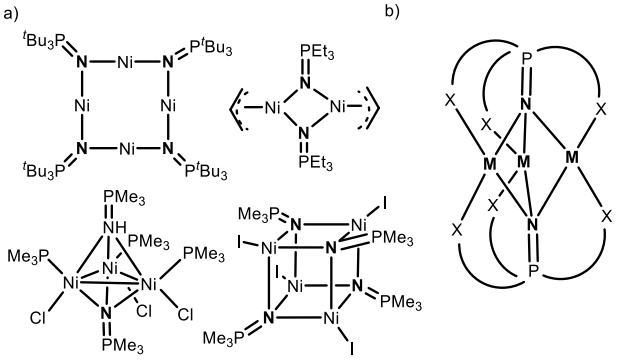

Figure 1. Multimetallic Ni complexes supported by phosphinimide ligands (a). Targeted design of multinucleating ligand taking advantage of the bridging propensity of phosphinimide (b).

Phenoxides were selected as pendant donors given their demonstrated ability to form robust complexes in conjunction with phosphinimine ligands.[12] The N-protonated phosphinimine, **$(O_3H_3PNH_2)^+$** (**2**), was prepared in quantitative yield through oxidation of the reported trisphenol phosphine,[13] **O_3H_3P** (**1**), with *o*-hydroxylaminesulfonic acid (Figure 2a). Given the precedent for phenoxide-phosphinimine motifs to support Ni complexes, we selected nickel to investigate the coordination chemistry with this new ligand framework. Targeting high oxidation state Ni is also of interest in the context of reactivity and spectroscopic studies relevant to water oxidation catalysis where Ni^{III} is invoked in metal oxides.[14] Several monometallic Ni^{III} complexes are known,[15] typically involving strong donors such as alkyl, aryl, and imido ligands. Among these examples, monometallic Ni salen[16] and

[a] *Department of Chemistry and Chemical Engineering, California Institute of Technology, Pasadena, California, 91125, USA*

†Electronic Supplementary Information (ESI) available: Synthetic procedures, spectroscopic data, crystallographic information. CCDC 1985597-1985598. For crystallographic data in COF format see DOI: 10.1039/x0xx00000x

phosphasalen[12a] complexes have been investigated. Substantial localization of the SOMO on the ligand is observed for the Ni salen complex, and conversely, a Ni^{III} complex is observed for the phosphasalen derivative.[1d, 16] A trinuclear Ni complex with distal metals bound to a triplesalen ligand was reported to access Ni^{III} upon electrochemical oxidation .[17] Heterometallic[18], dinuclear[19] and limited examples of homometallic complexes[20] displaying high oxidation state Ni are known; however, oxidized triangular Ni clusters with proximal metal centers supported by multi nucleating ligands remain rare.

Deprotonation of the phenols and phosphinimine was perfor med with excess KO^{t}Bu. The changes in the protonation state of the R_3PN motif were followed by $^{31}P\{^1H\}$ NMR spectroscopy. An additional peak is observed after the addition of two equivalents of KO^{t}Bu, presumably generating K_2SO_4 and the neutral trisphenol phosphinimine. Additional equivalents of KO^{t}Bu deprotonate the phenols first. However, two broad resonances are observed until a total of 10 equivalents of KO^{t}Bu have been added which suggests a mixture of species, likely due to different levels of K^+ coordination (Figure S8). Subsequent addition of 1.5 equivalents $NiBr_2$-DME leads to the isolation of a dark red material. A single crystal X-ray diffraction study (XRD) reveals the generation of a trinuclear metal complex supported by two phosphinimide-trisphenoxide ligands (Figure 2b), **$2K^+[(O_3PN)_2Ni_3]^{2-}$(3).** The phosphinimide binds in the desired μ_3 fashion while the phenoxides are terminal, generating a structure that is *pseudo*-C_3 symmetric. The trinickel complex is dianionic, with two K cations coordinated to the phenoxides, neutralizing the charge. Each Ni center displays a distorted square planar geometry with the sum of angles around Ni of 360°. The Ni-N distances in the range of 1.850(2)-1.865(2) Å are shorter than other four-coordinate Ni distances to bridging phosphinimide N (1.90-2.05 Å),[1f, 2c, d, 11b, 21] likely due to the chelating phenoxide donors. The three Ni centers display metal-metal distances in the range of 2.5744(7)-2.6546(9) Å, which are similar to Ni-Ni distances reported for diamond core bridged dinickel(II) complexes, especially for cases where the bridging atoms are O or N and the metals centers are not both coplanar with the bridges.[22] The nature of the solution structure was interrogated by NMR spectroscopy. The observation of relatively sharp resonances in the diamagnetic NMR chemical shift range indicates the diamagnetic nature of **3-DME**, consistent with the isolated Ni^{II} square planar centers being low spin, as expected.[23] The ^1H NMR spectrum in C_6D_6 features six *tert*-butyl resonances and four aromatic resonances, some of which are broad. Two nearly coincident resonances corresponding to bound DME are also observed. In the conditions used to obtain the solid-state structure hexamethyldisiloxane displaces the DME; however, **3-DME** is used for all other characterization and further reaction. The number of peaks, larger than expected for a C_3 structure (two for the *tert*-butyl and two for the arene groups), is consistent with the potassium cations being coordinated in solution and lowering the symmetry of the cluster.

Cyclic voltammetry studies of compound **3-DME** reveal two pseudo reversible oxidation events at -0.80 V and +0.05 V at 250 mV/s, with respect to Cp_2Fe/Cp_2Fe^+ (Figure S9). These are assigned to formal oxidations by one and two electrons, respectively, $Ni^{II}_2Ni^{III}/Ni^{II}_3$ and $Ni^{II}Ni^{III}_2/Ni^{II}_2Ni^{III}$. In comparison to the mononuclear Ni salen and phosphasalen complexes, the first oxidation event is much more facile (+0.58V, and +0.16 V, respectively).[1d, 16] The first oxidation event of **3-DME** is also more facile than the trinuclear triplesalen complex with distal metals (+0.22 V).[17] The more than 800 mV difference toward accessing the oxidized species is likely a consequence of the negative charge of the cluster and the more electron rich phosphinimide donor, despite its bridging nature, relative to the imine and phosphinimine. Treatment of **3-DME** with two equivalents of the weak oxidant, decamethyl ferrocenium triflate, results in the formation of a new, dark brown species,

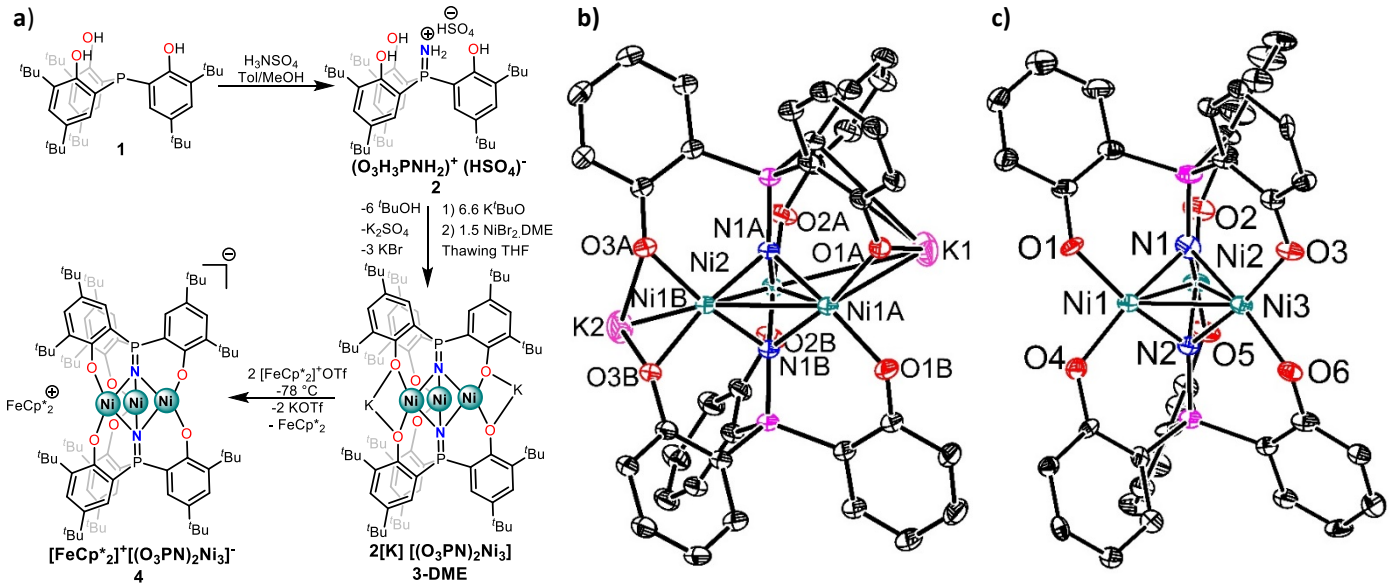

Figure 2: Synthesis of **2**, **3-DME**, and **4** (a). Solid-state structure of **3** (b) and **4** (c). Most carbons and hydrogens of ligand excluded for clarity. Selected bond lengths for **3**, Ni(1A)-Ni(1B) 2.5744(7) Å, Ni(1)-Ni(2) 2.6546(9) Å, Ni(1A)-N(1A) 1.850(2) Å, Ni(1B)-N(1A) 1.855(2) Å, Ni(2)-N(1A) 1.865(2) Å, Ni(1A)-O(1A) 1.902(2) Å, Ni(1A)-O(1B) 1.880(2) Å, Ni(2)-O(2A) 1.893(2) Å; and **4**, Ni(1)-Ni(3) 2.477(2) Å, Ni(1)-Ni(2) 2.636(2) Å, Ni(2)-Ni(3) 2.657(2) Å, Ni(1)-N(1) 1.856(7) Å, Ni(2)-N(1) 1.863(6) Å, Ni(3)-N(1) 1.869(7) Å, Ni(1)-N(2) 1.853(7) Å, Ni(2)-N(2) 1.863(6) Å, Ni(3)-N(2) 1.864(6) Å, Ni(1)-O(1) 1.880(5) Å, Ni(1)-O(4) 1.859(6) Å, Ni(2)-O(2) 1.887(6) Å, Ni(2)-O(5) 1.890(6) Å, Ni(3)-O(3) 1.879(6) Å, Ni(3)-O(6) 1.859(6) Å.

characterized as $[FeCp^*_2]^+(O_3PN)_2Ni_3]^-$(**4**).

The solid-state structure of **4** (Figure 2c) displays similar connectivity to $[(O_3PN)_2Ni_3]^{2-}$ (**3**). The two K cations are replaced with one outer-sphere decamethylferrocenium ($[Cp^*_2Fe]^+$). All Ni centers are still in a slightly distorted square planar geometry. There is a significant Ni-Ni contraction for one of the bonds with a bond distance of 2.477(2) Å (Ni(1)-Ni(3)), while the remaining Ni-Ni distances (2.657(2) Å and 2.636(2) Å) are in the range of those observed for **3**. The Ni-N distances are nearly identical to **3** ranging from 1.856(7) to 1.867(7) Å. There is a slight decrease of the Ni-O bond lengths (1.859(6)-1.890(6) Å for **4** vs 1.880(2)-1.893(2) Å for **3**), which could be due to an increase in the oxidation state at Ni or the removal of the K cations. Notably, the shorter Ni-O distances are located on Ni(1) and Ni(3) which are the metal centers with a shorter metal-metal distance suggesting that the oxidation is located at these two sites. Cyclic voltammetry studies were undertaken on **4** for comparison to **3-DME**. An oxidation and a reduction corresponding to the same redox processes observed for **3** are detected (Figure 3), assigned to $Ni^{II}Ni^{III}_2/Ni^{II}_2Ni^{III}$ and $Ni^{II}_2Ni^{III}/Ni^{II}_3$, respectively. Additionally, a reduction wave corresponding to the $[Cp^*_2Fe]^+/Cp^*_2Fe$ couple is observed. While the $Ni^{II}Ni^{III}_2/Ni^{II}_2Ni^{III}$ couple appears at the same potential for **3-DME** and **4**, the $Ni^{II}_2Ni^{III}/Ni^{II}_3$ is shifted (-800 mV in **3** vs -770 mV in **4**), suggesting that the K cations remain associated to the Ni_3 cluster in solution, consistent with the NMR data. Addition of KOTf to solutions of **4** did not result in a shift in the waves in the cyclic voltammograms, which may be due to slow association of K^+ to the monoanion. The shift in potential between **3-DME** and **4** is reminiscent of previously reported effects of redox inactive cations affecting transition metal or cluster potentials through Lewis acidity or charge effects.[24]

Compound **4** was further characterized by Evans method, NMR spectroscopy, and EPR. The Evans method produced a magnetic susceptibility value of 2.80 μ_B, which is close but higher than the expected value of 2.45 μ_B for two uncoupled unpaired electrons, for the combination of a S = 1/2 $\mathbf{[(O_3PN)_2Ni_3]^-}$ ion and the S = 1/2 $[Cp^*_2Fe]^+$ cation (assuming g=2.00).[25] Conversely, treating $\mathbf{[FeCp^*_2]^+}$ $\mathbf{[(O_3PN)_2Ni_3]^-}$ as an S = 3/2 system in combination with $[Cp^*_2Fe]^+$ results in an expected

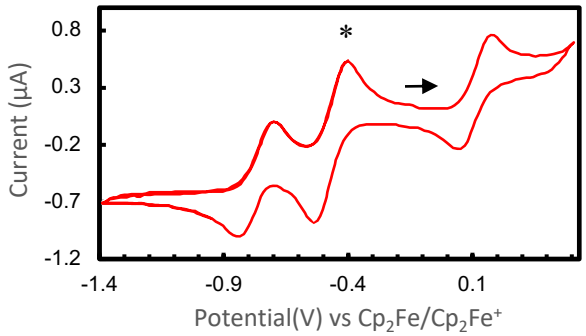

Figure 3: Cyclic voltammogram of **4** at a scan rate of 25 mV/s in THF. *Redox couple for $[Cp^*_2Fe]^+$/ Cp^*_2Fe.

μ_{eff} of 4.28 μ_B, a significant deviation from the observed value. Though **4** bears half-integer spin, ^{1}H NMR data for the cluster is minimally shifted, with chemical shifts ranging from -0.23 to 9.50 ppm, which are not significantly broadened, with $W_{1/2}$ ranging from 20 to 40 Hz; the decamethyl ferrocenium cation displays a single resonance in the paramagnetic region at -37.1 ppm. The chemical shift range is somewhat comparable to the Ni^{III}-phosphasalen ^{1}H NMR spectrum window (δ 1.6-19).[12a] The minimal broadness in the resonances of the ^{1}H NMR suggests a minimal contact mechanism contribution.[26]

To further characterize **4** and investigate whether the unpaired electron is metal or ligand-based, X-Band EPR studies were conducted. At 10 K, a *pseudo*-axial spectrum is observed with g_{par} of 2.51 and g_{perp} of 2.03 (Figure 4). Increasing the temperature above 30 K resulted in the loss of signal, in contrast with a previously reported salen system that shows different signals at low (rhombic signal, g_{ave}=2.18) vs high temperatures (isotropic signal, g_{iso}=2.04) consistent with tautomerism

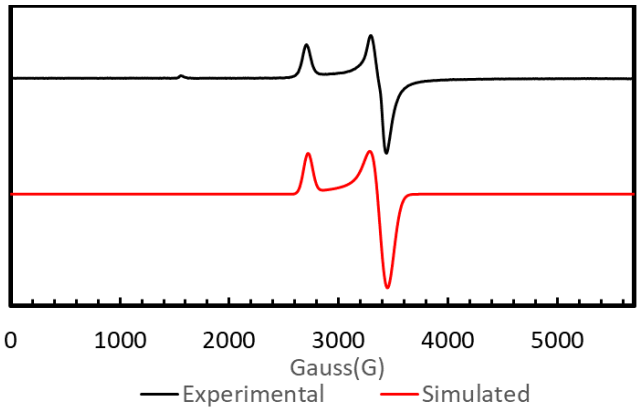

Figure 4: X-Band EPR spectrum of **4** (2 mM solid glass in 2-MeTHF, 10 K)

between Ni^{III} and oxidized phenoxide.[27] The behavior of **4** indicates that the Ni^{III} state is preferred relative to a ligand-based oxidation. The structural changes observed upon oxidation are in agreement with this assignment. The shortening of the Ni-Ni distance is indicative of an electronic change at the metal. Square planar d^8 metal complexes can support metal-metal bonds along the z vector; these interactions are strengthened upon oxidation, which removes an electron from an orbital with partial antibonding character (Figure S18).[28]

Computational studies of **3** and **4** were undertaken to further interrogate the electronic structure. Good agreement is observed between the structural parameters from XRD and computation (Table S2 and S3). The Ni(1)-Ni(3) contraction observed in **4** was also reproduced and was evaluated as an indication of oxidation at these metal sites. A higher Löwdin bond order is observed for Ni(1)-Ni(3) (0.43) than the other two Ni-Ni interactions (0.31). Analysis of Mulliken spin population shows significant spin density on Ni(1) and Ni(3), encompassing nearly 80% of unpaired spin, corroborating a metal-centered unpaired electron in **4**, as suggested by the EPR data (Table S4). These observations are consistent with a singly occupied molecular orbital that is antibonding with respect to the Ni(1)-Ni(3) interaction and non-bonding with respect to the Ni(1)-Ni(2) and Ni(3)-Ni(2) (Figure S18).

In summary, a new ligand platform for the rational synthesis of trinuclear clusters that takes advantage of the bridging ability of the phosphinimide motif has been described. Upon oxidation of a Ni^{II}_3 complex, this ligand supports a new example of a high-oxidation state Ni cluster, with a formal metal core oxidation state of $Ni^{II}_2Ni^{III}$. Notably, the Ni^{III} species is accessible at very

mild potentials (-800 mV vs Cp_2Fe^+/Cp_2Fe), likely a consequence of the high negative charge of the phosphinimide-trisphenoxide ligand and the electron rich phosphinimide donor. The reported clusters highlight the utility of the phosphinimide motif for the rational design of multidentate and multinucleating ligands for transition metals.

We thank Lawrence M. Henling and Mike Takase for crystallographic asistance and Paul H. Oyala for X-Band EPR assistance. The authors are grateful to the Natural Sciences and Engineering Research Counsel of Canada (MMS), Dow (TA), and the NSF (NSF-1531940 for EPR instrumentation) for financial support.

Conflicts of interest

The authors declare no competing financial interest

Notes and references

1. (a) Suzuki, H. *Eur. J. Inorg. Chem.* **2002,** *2002*, 1009-1023; (b) Hu, S.; Shima, T.; Hou, Z. *Nature* **2014,** *512*, 413; (c) Shima, T.; Hu, S.; Luo, G.; Kang, X.; Luo, Y.; Hou, Z. *Science* **2013,** *340*, 1549-1552; (d) Shoshani, M. M.; Johnson, S. A. *Nature Chemistry* **2017,** *9*, 1282; (e) Lee, Y.; Sloane, F. T.; Blondin, G.; Abboud, K. A.; García-Serres, R.; Murray, L. J. *Angew. Chem. Int. Ed.* **2015,** *54*, 1499-1503; (f) Camacho-Bunquin, J.; Ferguson, M. J.; Stryker, J. M. *J. Am. Chem. Soc.* **2013,** *135*, 5537-5540.
2. (a) Blondin, G.; Girerd, J. J. *Chem. Rev.* **1990,** *90*, 1359-1376; (b) Siegbahn, P. E. *Inorg. Chem.* **2000,** *39*, 2923-2935; (c) Klein, H. F.; Haller, S.; Koenig, H.; Dartiguenave, M.; Dartiguenave, Y.; Menu, M. J. *J. Am. Chem. Soc.* **1991,** *113*, 4673-4675; (d) Muller, U.; Bock, O.; Sippel, H.; Grob, T.; Dehnicke, K.; Greiner, A. *Z. Anorg. Allg. Chem.* **2002,** *628*, 1703-1707.
3. (a) Blakemore, J. D.; Crabtree, R. H.; Brudvig, G. W. *Chem. Rev.* **2015,** *115*, 12974-13005; (b) Tsui, E. Y.; Kanady, J. S.; Agapie, T. *Inorg. Chem.* **2013,** *52*, 13833-13848.
4. (a) Kanady, J. S.; Tsui, E. Y.; Day, M. W.; Agapie, T. *Science* **2011,** *333*, 733-736; (b) Reed, C.; Agapie, T. *J. Am. Chem. Soc.* **2019**; (c) Lionetti, D.; Day, M. W.; Agapie, T. *Chemical science* **2013,** *4*, 785-790; (d) Zhao, Q.; Betley, T. A. *Angew. Chem. Int. Ed.* **2011,** *50*, 709-712.
5. (a) Ferreira, R. B.; Murray, L. J. *Acc. Chem. Res.* **2019,** *52*, 447-455; (b) Murray, L. J.; Weare, W. W.; Shearer, J.; Mitchell, A. D.; Abboud, K. A. *J. Am. Chem. Soc.* **2014,** *136*, 13502-13505; (c) Powers, T. M.; Fout, A. R.; Zheng, S.-L.; Betley, T. A. *J. Am. Chem. Soc.* **2011,** *133*, 3336-3338.
6. Ermert, D. M.; Ghiviriga, I.; Catalano, V. J.; Shearer, J.; Murray, L. J. *Angew. Chem. Int. Ed.* **2015,** *54*, 7047-7050.
7. (a) Powers, T. M.; Betley, T. A. *J. Am. Chem. Soc.* **2013,** *135*, 12289-12296; (b) Eames, E. V.; Betley, T. A. *Inorg. Chem.* **2012,** *51*, 10274-10278.
8. (a) Reed, C. J.; Agapie, T. *J. Am. Chem. Soc.* **2019,** *141*, 9479-9484; (b) Kanady, J. S.; Mendoza-Cortes, J. L.; Tsui, E. Y.; Nielsen, R. J.; Goddard III, W. A.; Agapie, T. *J. Am. Chem. Soc.* **2013,** *135*, 1073-1082; (c) Lee, H. B.; Shiau, A. A.; Oyala, P. H.; Marchiori, D. A.; Gul, S.; Chatterjee, R.; Yano, J.; Britt, R. D.; Agapie, T. *J. Am. Chem. Soc.* **2018,** *140*, 17175-17187.
9. (a) Palumbo, C. T.; Zivkovic, I.; Scopelliti, R.; Mazzanti, M. *J. Am. Chem. Soc.* **2019**; (b) Rice, N. T.; Popov, I. A.; Russo, D. R.; Bacsa, J.; Batista, E. R.; Yang, P.; Telser, J.; La Pierre, H. S. *J. Am. Chem. Soc.* **2019,** *141*, 13222-13333; (c) Rice, N. T.; Su, J.; Gompa, T. P.; Russo, D. R.; Telser, J.; Palatinus, L.; Bacsa, J.; Yang, P.; Batista, E. R.; La Pierre, H. S. *Inorg. Chem.* **2019,** *58*, 5289-5304.
10. Ye, M.; Thompson, N. B.; Brown, A. C.; Suess, D. L. *J. Am. Chem. Soc.* **2019**.
11. (a) Bunquin, J. **2013**; (b) Nkala, F. M. **2017**.
12. (a) Cao, T. P. A.; Nocton, G.; Ricard, L.; Le Goff, X. F.; Auffrant, A. *Angew. Chem. Int. Ed.* **2014,** *53*, 1368-1372; (b) Bakewell, C.; Cao, T.-P.-A.; Long, N.; Le Goff, X. F.; Auffrant, A.; Williams, C. K. *J. Am. Chem. Soc.* **2012,** *134*, 20577-20580.
13. Liang, L.-C.; Chou, K.-W.; Su, W.-J.; Chen, H.-S.; Hsu, Y.-L. *Inorg. Chem.* **2015,** *54*, 11526-11534.
14. (a) Bates, M. K.; Jia, Q.; Doan, H.; Liang, W.; Mukerjee, S. *ACS Catalysis* **2016,** *6*, 155-161; (b) Hunter, B. M.; Thompson, N. B.; Müller, A. M.; Rossman, G. R.; Hill, M. G.; Winkler, J. R.; Gray, H. B. *Joule* **2018,** *2*, 747-763.
15. (a) Kogut, E.; Wiencko, H. L.; Zhang, L.; Cordeau, D. E.; Warren, T. H. *J. Am. Chem. Soc.* **2005,** *127*, 11248-11249; (b) Iluc, V. M.; Miller, A. J.; Anderson, J. S.; Monreal, M. J.; Mehn, M. P.; Hillhouse, G. L. *J. Am. Chem. Soc.* **2011,** *133*, 13055-13063; (c) Bour, J. R.; Camasso, N. M.; Meucci, E. A.; Kampf, J. W.; Canty, A. J.; Sanford, M. S. *J. Am. Chem. Soc.* **2016,** *138*, 16105-16111; (d) Lee, H.; Börgel, J.; Ritter, T. *Angew. Chem. Int. Ed.* **2017,** *56*, 6966-6969; (e) Zheng, B.; Tang, F.; Luo, J.; Schultz, J. W.; Rath, N. P.; Mirica, L. M. *J. Am. Chem. Soc.* **2014,** *136*, 6499-6504; (f) Pandarus, V.; Zargarian, D. *Chem. Commun.* **2007**, 978-980; (g) Spasyuk, D. M.; Zargarian, D.; van der Est, A. *Organometallics* **2009,** *28*, 6531-6540; (h) Lipschutz, M. I.; Yang, X.; Chatterjee, R.; Tilley, T. D. *J. Am. Chem. Soc.* **2013,** *135*, 15298-15301; (i) Zhang, C.-P.; Wang, H.; Klein, A.; Biewer, C.; Stirnat, K.; Yamaguchi, Y.; Xu, L.; Gomez-Benitez, V.; Vicic, D. A. *J. Am. Chem. Soc.* **2013,** *135*, 8141-8144; (j) Bour, J. R.; Ferguson, D. M.; McClain, E. J.; Kampf, J. W.; Sanford, M. S. *J. Am. Chem. Soc.* **2019,** *141*, 8914-8920.
16. Storr, T.; Wasinger, E. C.; Pratt, R. C.; Stack, T. D. P. *Angew. Chem. Int. Ed.* **2007,** *46*, 5198-5201.
17. Glaser, T.; Heidemeier, M.; Fröhlich, R.; Hildebrandt, P.; Bothe, E.; Bill, E. *Inorg. Chem.* **2005,** *44*, 5467-5482.
18. (a) Glaser, T.; Kesting, F.; Beissel, T.; Bill, E.; Weyhermüller, T.; Meyer-Klaucke, W.; Wieghardt, K. *Inorg. Chem.* **1999,** *38*, 722-732; (b) Kouno, M.; Yoshinari, N.; Kuwamura, N.; Yamagami, K.; Sekiyama, A.; Okumura, M.; Konno, T. *Angew. Chem.* **2017,** *129*, 13950-13954; (c) Beissel, T.; Birkelbach, F.; Bill, E.; Glaser, T.; Kesting, F.; Krebs, C.; Weyhermüller, T.; Wieghardt, K.; Butzlaff, C.; Trautwein, A. X. *J. Am. Chem. Soc.* **1996,** *118*, 12376-12390.
19. (a) Franolic, J. D.; Wang, W. Y.; Millar, M. *J. Am. Chem. Soc.* **1992,** *114*, 6587-6588; (b) Diccianni, J. B.; Hu, C.; Diao, T. *Angew. Chem.* **2017,** *129*, 3689-3693; (c) Lee, C.-M.; Chiou, T.-W.; Chen, H.-H.; Chiang, C.-Y.; Kuo, T.-S.; Liaw, W.-F. *Inorg. Chem.* **2007,** *46*, 8913-8923.
20. (a) Jacob, S. I.; Douair, I.; Wu, G.; Maron, L.; Ménard, G. *Chem. Commun.* **2020**; (b) Berry, J. F.; Cotton, F. A.; Daniels, L. M.; Murillo, C. A. *J. Am. Chem. Soc.* **2002,** *124*, 3212-3213; (c) North, T. E.; Thoden, J. B.; Spencer, B.; Dahl, L. F. *Organometallics* **1993,** *12*, 1299-1313.
21. (a) Krieger, M.; Gould, R. O.; Harms, K.; Greiner, A.; Dehnicke, K. *Z. Anorg. Allg. Chem.* **2001,** *627*, 747-754; (b) Müller, U.; Bock, O.; Sippel, H.; Gröb, T.; Dehnicke, K.; Greiner, A. *Z. Anorg. Allg. Chem.* **2002,** *628*, 1703-1707.
22. (a) Ölscher, F.; Göttker-Schnetmann, I.; Monteil, V.; Mecking, S. *J. Am. Chem. Soc.* **2015,** *137*, 14819-14828; (b) Soloshonok, V. A.; Ono, T.; Ueki, H.; Vanthuyne, N.; Balaban, T. S.; Bürck, J.; Fliegl, H.; Klopper, W.; Naubron, J.-V.; Bui, T. T. T.; Drake, A. F.; Roussel, C. *J. Am. Chem. Soc.* **2010,** *132*, 10477-10483; (c) Klein, H.-F.; Dal, A.; Hartmann, S.; Flörke, U.; Haupt, H.-J. *Inorg. Chim. Acta* **1999,** *287*, 199-203.
23. Gray, H. B.; Ballhausen, C. *J. Am. Chem. Soc.* **1963,** *85*, 260-265.
24. (a) Tsui, E. Y.; Agapie, T. *Proceedings of the National Academy of Sciences* **2013,** *110*, 10084-10088; (b) Tsui, E. Y.; Tran, R.; Yano, J.; Agapie, T. *Nature Chemistry* **2013,** *5*, 293-299; (c) Horak, K. T.; Lin, S.; Rittle, J.; Agapie, T. *Organometallics* **2015,** *34*, 4429-4432; (d) Reath, A. H.; Ziller, J. W.; Tsay, C.; Ryan, A. J.; Yang, J. Y. *Inorg. Chem.* **2017,** *56*, 3713-3718; (e) Chantarojsiri, T.; Reath, A. H.; Yang, J. Y. *Angew. Chem. Int. Ed.* **2018,** *57*, 14037-14042; (f) Kang, K.; Fuller, J.; Reath, A. H.; Ziller, J. W.; Alexandrova, A. N.; Yang, J. Y. *Chemical science* **2019,** *10*, 10135-10142; (g) Park, Y. J.; Ziller, J. W.; Borovik, A. *J. Am. Chem. Soc.* **2011,** *133*, 9258-9261.
25. Gray, H. B.; Hendrickson, D. N.; Sohn, Y. *Inorg. Chem.* **1971,** *10*, 1559-1563. Various ferrocenium salts have shown effective magnetic moments 0.25-0.89 μB greater than the expected value, which is in the range observed here.
26. Kurland, R. J.; McGarvey, B. R. *Journal of Magnetic Resonance (1969)* **1970,** *2*, 286-301.
27. Shimazaki, Y.; Tani, F.; Fukui, K.; Naruta, Y.; Yamauchi, O. *J. Am. Chem. Soc.* **2003,** *125*, 10512-10513.
28. Bercaw, J. E.; Durrell, A. C.; Gray, H. B.; Green, J. C.; Hazari, N.; Labinger, J. A.; Winkler, J. R. *Inorg. Chem.* **2010,** *49*, 1801-1810.

TOC Graphic

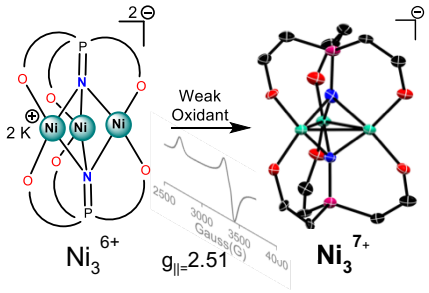

We report the synthesis of trinuclear Ni clusters supported by a tetraanionic trisphenolphosphinimde ligand. The dianionic $[(O_3PN)_2Ni_3]^{2-}$ cluster is oxidized at low potentials to form the monanionic $[(O_3PN)_2Ni_3]^{-}$ species, featuring Ni^{III} with proximal metal arrangement.